THE JOURNAL OF BIOLOGICAL CHEMISTRY VOL. 289, NO. 35, pp. 24079–24090, August 29, 2014

Structural Determinants of the Transient Receptor Potential 1 (TRPV1) Channel Activation by Phospholipid Analogs*[S]

Received for publication, May 5, 2014, and in revised form, July 10, 2014 Published, JBC Papers in Press, July 17, 2014, DOI 10.1074/jbc.M114.572503

Sara L. Morales-Lázaro[‡1], Barbara Serrano-Flores[‡1], Itzel Llorente[‡], Enrique Hernández-García[‡], Ricardo González-Ramírez[§], Souvik Banerjee[¶], Duane Miller[¶], Veeresh Gududuru[‖], James Fells[**], Derek Norman[**], Gabor Tigyi[**], Diana Escalante-Alcalde[‡], and Tamara Rosenbaum[‡2]

From the [‡]Departamento de Neurodesarrollo y Fisiología, División de Neurociencias, Instituto de Fisiología Celular, Universidad Nacional Autónoma de México, México D.F. 04510, México, the [§]Departmento de Biología Molecular e Histocompatibilidad, Hospital General "Dr. Manuel Gea González", México, D.F. 14080, México, the [¶]Department of Pharmaceutical Sciences, University of Tennessee Health Science Center, Memphis, Tennessee 38163, [‖]RxBio Inc., Memphis, Tennessee 38163, and the [**]Department of Physiology, University of Tennessee Health Science Center, Memphis, Tennessee 38163

Background: The TRPV1 ion channel can be regulated by negatively charged lipids.
Results: TRPV1 shows specificity for LPA analogs containing monounsaturated hydrocarbon chains with a negatively charged phosphate, cyclic phosphate, and thiophosphate headgroup.
Conclusion: TRPV1 activation is highly restricted to natural lipids with oleyl or oleoyl side chains.
Significance: Production of endogenous C18:1 lysophospholipids can selectively trigger activation of TRPV1 and nociceptive neuronal responses.

The transient receptor potential vanilloid 1 (TRPV1) ion channel is a polymodal protein that responds to various stimuli, including capsaicin (the pungent compound found in chili peppers), extracellular acid, and basic intracellular pH, temperatures close to 42 °C, and several lipids. Lysophosphatidic acid (LPA), an endogenous lipid widely associated with neuropathic pain, is an agonist of the TRPV1 channel found in primary afferent nociceptors and is activated by other noxious stimuli. Agonists or antagonists of lipid and other chemical natures are known to possess specific structural requirements for producing functional effects on their targets. To better understand how LPA and other lipid analogs might interact and affect the function of TRPV1, we set out to determine the structural features of these lipids that result in the activation of TRPV1. By changing the acyl chain length, saturation, and headgroup of these LPA analogs, we established strict requirements for activation of TRPV1. Among the natural LPA analogs, we found that only LPA 18:1, alkylglycerophosphate 18:1, and cyclic phosphatidic acid 18:1, all with a monounsaturated C18 hydrocarbon chain activate TRPV1, whereas polyunsaturated and saturated analogs do not. Thus, TRPV1 shows a more restricted ligand specificity compared with LPA G-protein-coupled receptors. We synthesized fatty alcohol phosphates and thiophosphates and found that many of them with a single double bond in position Δ9, 10, or 11 and Δ9 cyclopropyl group can activate TRPV1 with efficacy similar to capsaicin. Finally, we developed a pharmacophore and proposed a mechanistic model for how these lipids could induce a conformational change that activates TRPV1.

The transient receptor potential vanilloid 1 (TRPV1)[3] is a member of the TRP channel family of ion channels that has been widely associated with painful processes such as angina pectoris, arthritis, and cancer, as well as inflammatory events (1–5). The activation of this receptor in the peripheral sensory cells where it is expressed leads to pain perception (6, 7).

This polymodal ion channel is activated by various stimuli that include low extracellular and high intracellular pH, pungent compounds found in some plants, high temperatures (8) and lipids such as lysophosphatidic acid 18:1 (LPA) (9).

LPA is found in serum and plasma, and it can reach up to micromolar concentrations in biological fluids (10, 11). LPA has been importantly linked to neuropathic pain, and for several years it was thought to produce it solely through its interaction with specific GPCRs (LPA_{1-6}) (12, 13), with the LPA_1 receptor being particularly important in this process (14). Recently, our group demonstrated a direct and physiologically relevant interaction of TRPV1 with LPA. By using a combination of electrophysiological and biochemical techniques, we showed that LPA 18:1 and the bromophosphonate analog of LPA (BrP-LPA), which is an antagonist of several of the LPA receptors, activate TRPV1 through a direct interaction with the

* This work was supported, in whole or in part, by National Institutes of Health Grant CA-092160 (to G. T.). This work was also supported by grants from Programa de Apoyo a Proyectos de Investigación e Innovación Tecnológica (PAPIIT) IN204111, Consejo Nacional de Ciencia y Tecnologia 129474, Fundación Miguel Alemán and Fundación Marcos Moshinsky (to T. R.), Consejo Nacional de Ciencia y Tecnologia Grant 165897 (to D. E.-A.), Grant U01-AI-107331, the Van Vleet Endowment (to G. T.), and by Award I01BX007080 from the Biomedical Laboratory Research and Development Service of the Veterans Affairs Office of Research and Development (to G. T.)
[S] This article contains supplemental methods.
[1] Both authors contributed equally to this work.
[2] To whom correspondence should be addressed. Tel.: 5255-5622-5624; Fax: 5255-5622-5607; E-mail: trosenba@ifc.unam.mx.

[3] The abbreviations used are: TRPV1, transient receptor potential vanilloid 1; LPA, lysophosphatidic acid; BrP-LPA, α-bromomethylene phosphonate LPA; DGPP, diacylglycerol pyrophosphate; CPA, cyclic phosphatidic acid; FAP, fatty acid phosphate/thiophosphate/boron phosphate; TRP, transient receptor potential; PDB, Protein Data Bank; PIP_2, phosphatidylinositol 4,5-bisphosphate; GPCR, G-protein-coupled receptor; AGP, alkylglycerophosphate; MOE, Molecular Operating Environment.

proximal C-terminal region of the ion channel, a site that is also occupied by phosphatidylinositol 4,5-bisphosphate (PIP_2) (9).

Finally, we were able to observe nocifensive behavior generation when we injected LPA into the paws of mice. This response was diminished in TRPV1 knock-out animals, indicating that LPA can produce acute pain through the activation of TRPV1 (9).

Mechanistically, we found that the neutralization of the positively charged residue Lys-710 in the C terminus of the protein rendered the mutant TRPV1-K710Q channels less sensitive to LPA, whereas when the charge was reversed (K710D), the channels were almost completely insensitive to the lipid, indicating that activation of the channel was partly dependent on an electrostatic interaction (9).

Another lipid that regulates the activity of TRPV1 is PIP_2 (15–18). The role of PIP_2 has been controversial, with one research group suggesting that PIP_2 is not necessary for recombinant purified TRPV1 activation in artificial liposomes (19). In fact, it has been shown that PIP_2 can inhibit TRPV1 function but under conditions where it is incorporated to the extracellular side of the plasma membrane (18). However, it is accepted that intracellular PIP_2 is necessary for the activation of TRPV1 by capsaicin in biological membranes (20, 21). Moreover, similar to what we had previously shown for LPA (9), several negatively charged lipids have been shown to positively regulate the activity of TRPV1 (16). We set out to determine the structural requirements for the activation of TRPV1 by lipids similar to LPA, some of which are naturally occurring lysophospholipids.

For other channel types and lipids, it has been shown that the length of the acyl chain, the presence or absence of unsaturations, as well as the nature of the headgroup charge linked with the acyl chain can influence the effect of these molecules on ion channel function. For example, M-type potassium channels are activated by a large variety of lipid phosphates with minimum requirements for acyl chain and the presence of a phosphate headgroup (22, 23).

In this study, we have evaluated the impact of the LPA structural motifs, the hydrocarbon chain, the glycerol backbone, and the phosphate headgroup, on the structure-activity relationship of TRPV1 activation, and we have delineated the minimum requirements for agonist activity in this family of compounds.

EXPERIMENTAL PROCEDURES

HEK293 Cell Culture and Recording—HEK293 cells expressing large T antigen were transfected with WT rTRPV1 or the TRPV1-K710D mutant together with pIRES-GFP (BD Biosciences) using JetPEI (Polyplus Transfection, Illkirch, France) following the suppliers' methods. Inside-out clamp recordings of TRPV1 were made using Ca^{2+}-free symmetrical solutions consisting of 130 mM NaCl, 3 mM HEPES (pH 7.2), and 1 mM EDTA. Solutions were changed with an RSC-200 rapid solution changer (BioLogic Science Instruments, Claix, France). The acyl forms of LPA 18:1, LPA 18:0, LPA 6:0, cyclic phosphatidic acid (CPA) 18:1, dioleoylglycerophosphate (DGPP) 18:1, and the ether lipid analogs of LPA alkylglycerophosphate (AGP) 18:1 and 16:0 were purchased from Avanti Polar Lipids, Inc. (Alabaster, AL); LPA 18:2 was purchased from Echelon Biosciences, Inc. (Salt Lake City, UT). Oleic acid and glycerol phosphate were purchased from Sigma. The fatty acid phosphates and thiophosphates (FAP) were synthesized as described in the supplemental methods (24), and FAP-1–11 analogs were synthesized as described previously (25). All lipids were prepared as 5 or 10 mM stocks in DMEM, 1% fatty acid-free BSA as reported previously (9). All stocks were frozen for a week, then sonicated during 30 min before use, and then diluted in recording solutions and resonicated in a Branson (Danbury, CT) 1510 sonicator.

Evoked currents from TRPV1-expressing HEK293 cells were low-pass filtered at 2.9 kHz and sampled at 10 kHz with an EPC 10 amplifier (HEKA Elektronik GmbH, Pfalz, Germany). Inside-out patches were held at 0 mV, and voltage was then stepped from 0 to −120 to 120 mV for 100 ms in 10-mV increments and then returned to 0 mV. All recordings were performed at room temperature (19 ± 3 °C). Currents obtained in the presence of the different lipids were normalized to the maximal current obtained with a saturating (4 μM) capsaicin concentration (I/I_{max}). To perform dose-response curves, a given concentration of the lipid was applied to a TRPV1-expressing membrane patch, and currents were measured and normalized to the maximal current obtained in the presence of 4 μM capsaicin. A single concentration of lipid was used to obtain the average for activation from several different membrane patches for each point in the dose-response curves, and then the data were fitted to the Hill equation, as described previously (26). Data were acquired and analyzed with PULSE software (HEKA Elektronik) and were plotted and analyzed with programs written using Igor Pro (WaveMetrics Inc., Portland, OR).

In Vitro Interaction Assays—Surface proteins were obtained from HEK293 cells transiently expressing TRPV1 channels using the cell surface isolation kit (Pierce) according to the manufacturer's instructions. For the overlay assay, lipids were dissolved in DMEM (Invitrogen) with 1% fatty acid-free BSA and prepared as 10 mM stocks and spotted (100 nmol/spot) onto a nitrocellulose membrane (GE Healthcare). The membrane was air-dried for 1 h at room temperature and blocked with PBS containing 10% nonfat dry milk and 1% fatty acid-free BSA for 2 h with gentle shaking. After washing twice with PBS, 0.05% Tween 20 (PBS-T), the membrane was incubated with the surface protein solution containing 10–20 μg of total surface protein in 50 mM Tris-HCl (pH 8), 150 mM NaCl, 0.5% IGEPAL® (Sigma), 1× complete protease inhibitor mixture (Roche Applied Science), and 0.5% BSA at 4 °C for 48 h with shaking. After three washes with PBS-T, the membranes were incubated with anti-TRPV1 antibody (1:500; sc-12498, P-19; Santa Cruz Biotechnology, Santa Cruz, CA) in PBS-T with 5% nonfat dry milk overnight at 4 °C. Finally, following three more washes with PBS-T, the membranes were incubated with horseradish peroxidase-conjugated secondary anti-goat antibody, and the binding of lipids to TRPV1 was visualized by chemiluminescence by exposing the blot for 15 min (Amersham Biosciences). For assays with LPA-coated beads, plasma membrane protein extracts were incubated with LPA beads or with control beads (Echelon Biosciences) for 2 h at 4 °C and washed five times with binding buffer containing 0.5% IGEPAL® (Sigma). For competition assays, protein extracts were previously incubated with 10 μM FAP-4 lipid for 2 h. Pro-

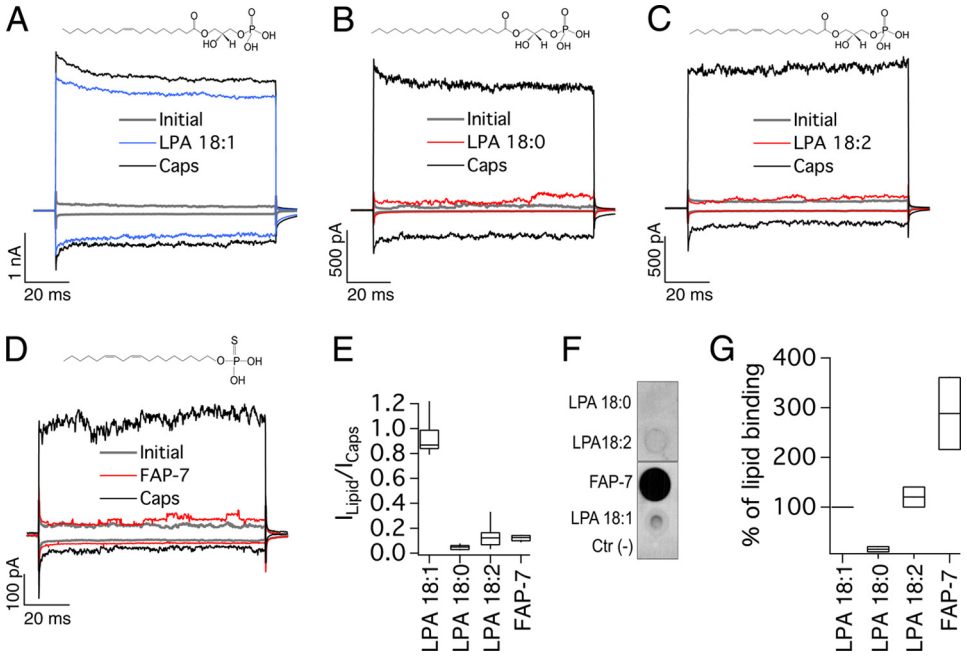

FIGURE 1. **Effects of saturated and unsaturated long-chain analogs of LPA on TRPV1 activation.** All representative traces were obtained at −120 and +120 mV. *A*, initially (leak, *gray*), after 4 μM capsaicin (*Caps*, *black*), and after a wash of capsaicin and with 5 μM LPA 18:1 for 5 min (*blue*). Currents were obtained from inside-out membrane patches expressing TRPV1. *B*, initially (in the absence of agonist, *gray*), after 5 min of 5 μM LPA 18:0 (*red*), and after 4 μM capsaicin (*Caps*, *black*). *C*, traces obtained initially (*gray*), after 5 μM LPA 18:2 (*red*), and after 4 μM capsaicin (*Caps*, *black*). *D*, initial currents are in *gray*, after 5 min of 5 μM FAP-7 compound (*red*), and after 4 μM capsaicin (*Caps*, *black*). *E*, box-plot of the activation of TRPV1 by the different lipids. The *horizontal line* within each box indicates the median; *boxes* show the 25th and 75th percentiles, and *whiskers* show the 5th and 95th percentiles of the data obtained at +120 mV and normalized to activation by 4 μM capsaicin ($n = 13$ for LPA 18:1, 6 for LPA 18:0, 20 for LPA 18:2 and 5 for FAP-7). *F*, overlay assay with WT TRPV1 protein to show the interaction of the channel with long-chain lipids LPA 18:2 and compound FAP-7. No signal is observed for LPA 18:0, whereas an increase in binding to the channel is observed with LPA 18:2 and compound FAP-7. DMEM with 1% fatty acid-free BSA was used as a negative control indicated as *Ctr* (−). *G*, densitometry was performed for the different lipid spots and normalized with respect to the positive control (LPA 18:1). Data are shown as in *E* ($n = 2$).

teins pulled down from each sample were eluted from the beads by adding an equal volume of 2× Laemmli sample buffer to the beads and heating to 95 °C for 5 min. Eluted proteins were separated by SDS-PAGE and analyzed by immunoblot assays using an anti-TRPV1 (sc-12498, P-19; Santa Cruz Biotechnology) antibody. In every experiment, a small sample of the total membrane protein extract was loaded to the gel as a positive control for TRPV1 protein expression (*lane 1* in Fig. 3*C*). Immunoblots were developed by ECL reagent, and densitometric analysis was done using ImageJ software (National Institutes of Health) and expressed as relative protein levels *versus* the amount of TRPV1 bound to LPA beads (9). Densitometric analysis for the overlay assays was performed also by using the ImageJ software, although these assays are not strictly quantitative.

Ligand-based TRPV1 Pharmacophore Modeling—The flexible alignment models were created with the Molecular Operating Environment (MOE) 2011.10 from Chemical Computing Group (Montreal, Canada). Active compounds were aligned with the flexible alignment module implemented in MOE using default parameters. The alignment with the lowest alignment score S and average strain energy score U were selected. The active alignment model was then fixed, and inactive compounds were separately aligned with the flexible alignment module using the same settings. The final conformation for each compound was selected on the basis of the compound's lowest energy strain and overlap of molecular features.

Pharmacophore modeling was performed using the pharmacophore query editor function in MOE. Models were manually created using the lowest energy conformation of the flexibly aligned models. The pharmacophore points (one anionic group and two hydrophobic groups) were identified as those structural features of the active compounds also sharing a common volume.

Molecular Modeling—Monte Carlo conformational analysis of lipids was carried out using the Multiple Minimum program in the MacroModel suite of software Version 9.7 (Schrödinger Inc., Surrey, UK). Coordinates of LPA 18:0, 18:1, and 18:2 were obtained from sdf files found at the PubChem database (CID: 9547179, 5311263, and 53478601). A 10,000-step conformational search was performed on the three molecules using the OPLS-2005 force field and the water solvation model (27). Conformers were selected using a 3.0 kcal/mol energy cutoff and pooled into geometrically similar families based on the root mean square difference between corresponding torsion angles in pairs of structures using XCluster.

Modeling of TRPV1-Lipid Interactions—The structures of monomers of the TRPV1 channel in either the closed (PDB code 3J5P-B) or open (PDB code 3J5Q-D) state were used as templates for docking the most abundant structural conformations of 18-carbon LPAs. Residues 361–719 were used in both cases because the binding of PIP_2 (17, 18, 21) and LPA (9) has been found to occur on the proximal C terminus, which was also supported by molecular modeling experiments (28). Structures were prepared in Autodock Tools, and all the dockings were carried out with Autodock 4.2 (29) with a Lamarckian

TABLE 1
Summary of the pharmacological profile of lipids and role on TRPV1 activity

Lipid	Chemical Nomenclature	Structure	pK_a*	logP**	I_{lipid}/I_{max} (%)
LPA 18:1	(*R*)-2-hydroxy-3-(phosphonooxy)propyl oleate	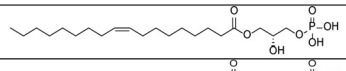	6.31	6.12	93
LPA 18:0	(*R*)-2-hydroxy-3-(phosphonooxy)propyl stearate	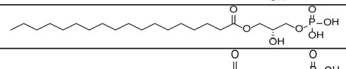	6.31	6.38	5 [8]
LPA 18:2	(9*Z*,12*Z*)-(*R*)-2-hydroxy-3-(phosphonooxy)propyl octadeca-9, 12-dienoate	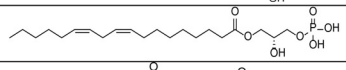	6.31	5.86	8 [13]
LPA 6:0	(*R*)-2-hydroxy-3-(phosphonooxy)propyl hexanoate	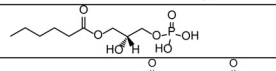	6.31	1.62	8
BrP-LPA	((3*S*)-1-bromo-3-hydroxy-4-(palmitoyloxy)butyl) phosphonic acid	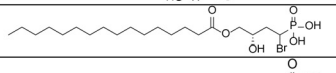	6.55	5.91	90
AGP 18:1	(*R*,*Z*)-2-hydroxy-3-(octadec-9-en-1-yloxy)propyl dihydrogen phosphate	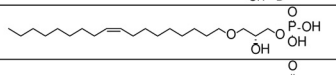	6.31	6.45	94
AGP 18:0	(*R*)-2-hydroxy-3-(octadecyloxy)propyl dihydrogen phosphate	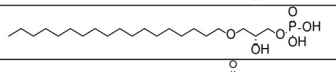	6.34	6.71	13
CPA 18:1	((4*S*)-2-hydroxy-2-oxido-1,3,2-dioxaphospholan-4-yl)methyl oleate	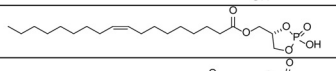	4.04	6.41	97
CPA 16:0	(2-hydroxy-2-oxido-1,3,2-oxaphospholan-5-yl)methyl palmitate	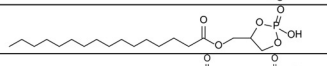	4.04	5.29	12
DGPP 18:1	(*Z*)-(*R*)-3-(phophonooxy)-propane-1,2-dyil dioleate	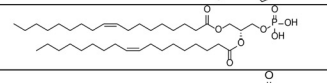	6.26	12.5	1
Oleic Acid	(9*Z*)-Octadec-9-enoic acid	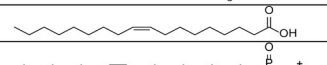	4.88	6.29	1
FAP-1	(*Z*)-octadec-9-en-1-yl phosphate	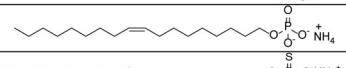	6.46	6.99	88
FAP-3	ammonium (*E*)-*O*-octadec-9-en-1-yl *O*-hydrogenphosphorothioate	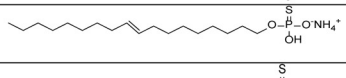	4.96	7.72	91
FAP-4	ammonium (*Z*)-*O*-octadec-11-en-1-yl *O*-hydrogenphosphorothioate	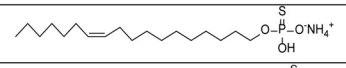	4.96	7.72	81
FAP-5	ammonium (*Z*)-*O*-nonadec-10-en-1-yl *O*-hydrogenphosphorothioate	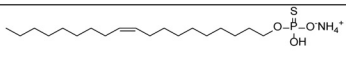	4.96	8.12	80
FAP-6	ammonium (*Z*)-*O*-icos-11-en-1-yl *O*-hydrogenphosphorothioate	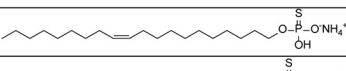	4.96	8.51	87
FAP-7	ammonium *O*-(9*Z*,12*Z*)-octadeca-9,12-dien-1-yl *O*-hydrogenphosphorothioate	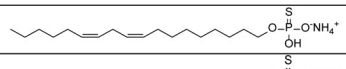	6.46	7.46	12
FAP-8	ammonium (*O*)-(8-(2-octylcyclopropyl)octyl) *O*-hydrogenphosphorothioate	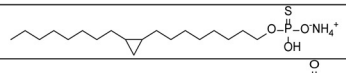	4.96	7.74	94
FAP-9	(*Z*)-(hydroxy(octadec-9-en-1-yloxy)phosphoryl)trihydroborate	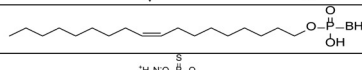	2.24	6.99	10
FAP-10	ammonium *O*-(2-(4,4-dimethylpentan-2-yl)-5,7,7-trimethyloctyl) *O*-hydrogenphosphorothioate	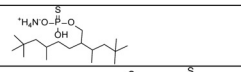	5.02	7.8	6
FAP-11	ammonium (Z)-*O*-(2-(octadec-9-en-1-yloxy)ethyl) *O*-hydrogenphosphorothioate	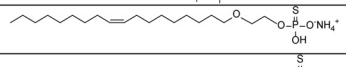	4.89	7.56	13 [7]
FAP-12	ammonium (Z)-*O*-(3-(octadec-9-en-1-yloxy)propyl) *O*-hydrogenphosphorothioate	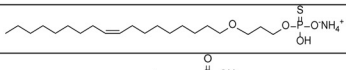	4.93	7.61	81
FAP-14	(*E*)-hex-3-en-1-yl dihydrogen phosphate	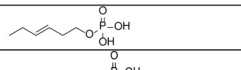	6.43	2.23	9
FAP-15	octyl dihydrogen phosphate	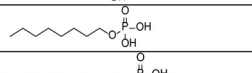	6.46	3.28	3
FAP-16	decyl dihydrogen phosphate	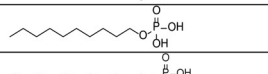	6.46	4.08	7
FAP-17	dodecyl dihydrogen phosphate	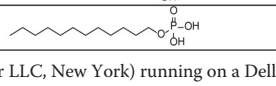	6.46	4.87	4

* The pK_a calculations were performed utilizing Molecular Modeling Suite 2011 (Schrödinger LLC, New York) running on a Dell Linux work station. pK_a values are calculated at pH 7 in water.

** The logP (partition coefficient) calculations were performed utilizing ChemDraw® Pro Suite running on a Dell Windows 7 workstation. Numbers in parentheses were obtained at a concentration of 25 μM. All other values were obtained at a concentration of 5 μM.

genetic algorithm allowing flexibility to Lys-710 and the lipids. Figures were prepared in PyMOL with the Autodock/Vina plugin (30).

Statistical Analysis—Statistical comparisons were made with a one-way analysis of variance test. $p < 0.05$ was considered statistically significant. Group data are reported as the mean ± S.E.

RESULTS

TRPV1 Channel Is Activated by Lipids Similar to LPA—Our approach to a comprehensive study of the structural requirements of the lipid ligands necessary to activate TRPV1 was based on the designation of five motifs in the LPA scaffold as follows: 1) the glycerol backbone and its substitutions; 2) the

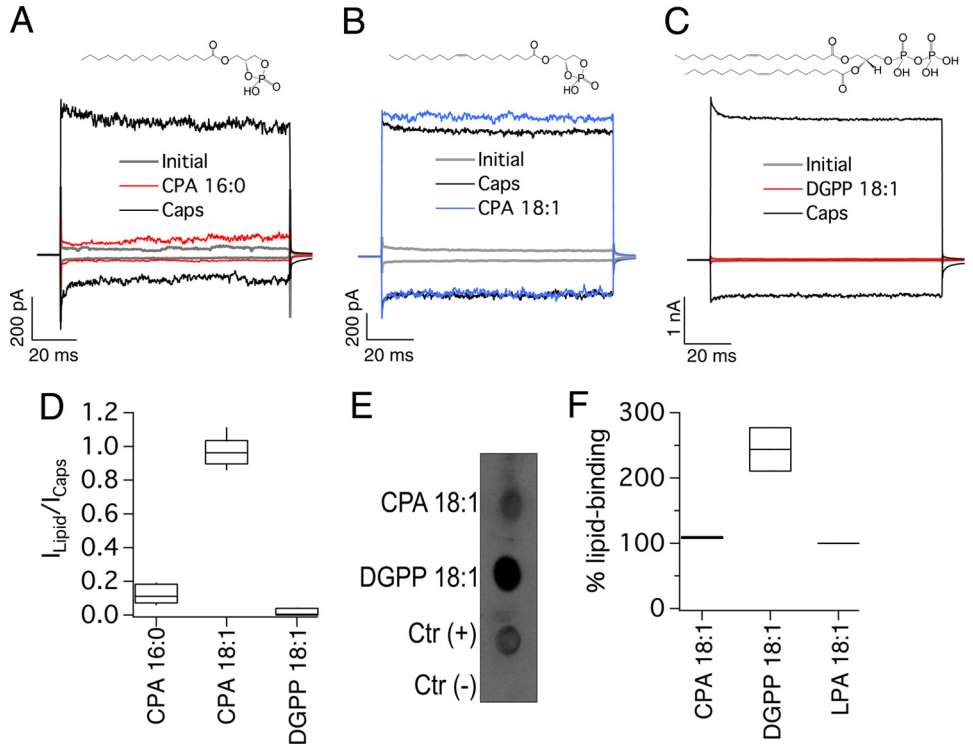

FIGURE 2. **Effects of cyclic phosphates and DGPP on TRPV1 function.** All representative traces were obtained at −120 and +120 mV. *A,* initially (leak, *gray*), after 4 μM capsaicin (*Caps, black*), and after wash of capsaicin and with 5 μM CPA 16:0 for 5 min (*red*). Currents were obtained from inside-out membrane patches expressing TRPV1. *B, gray* is the initial current, *black* is 4 μM capsaicin (*Caps*), and *blue* is after 5 min of 5 μM CPA 18:1. *C, gray* is the initial current; *black* is 4 μM capsaicin, and *red* is after 5 min of 5 μM DGPP 18:1. The chemical structures of each lipid used are shown above the current traces. *D, horizontal line* within each box indicates the median; *boxes* show the 25th and 75th percentiles, and *whiskers* show the 5th and 95th percentiles of the data obtained at +120 mV and normalized to activation by 4 μM capsaicin. Capsaicin ($n = 5$ for CPA 16:0, 6 for CPA 18:1, and 6 for DGPP 18:1). *E,* overlay assay shows that CPA18:1 and DGPP 18:1 bind to wild type (*WT*) TRPV1. DMEM with 1% fatty acid-free BSA was used as a negative control indicated as *Ctr*(−). *F,* densitometry was performed for the different lipid spots and normalized with respect to the positive control (LPA 18:1). Data are shown as in *D* ($n = 2$).

bond of the hydrocarbon chain to the headgroup; 3) the position and number of double bonds in the hydrocarbon chain; 4) the length of the hydrocarbon chain, and 5) the nature of the negatively charged headgroup. As shown previously (9), LPA 18:1 (5 μM) activated TRPV1 currents nearly as efficiently as 4 μM capsaicin (Fig. 1, *A* and *E*).

To begin to determine the nature of the requirements for activation of TRPV1 by LPA, we investigated what effect the lack of a double bond or the presence of more than one double bond in the hydrocarbon chain would have on TRPV1 activation. For this purpose, we used commercially available saturated LPA 18:0 (5 μM) and LPA 18:2 (5 μM). To our surprise, although structurally similar to LPA 18:1, both LPA 18:0 and LPA 18:2 failed to activate the channel (Fig. 1, *B* and *C, red traces,* and *E*). Moreover, FAP-7, a synthetic analog with an 18:2 fatty alcohol chain also failed to activate TRPV1 (Fig. 1, *D, red trace,* and *E*), consistent with the result we obtained with LPA 18:2. Additionally, both LPA 18:0 and LPA 18:2 failed to activate TRPV1 even at concentrations as high as 25 μM (Table 1), the highest concentration we could use without breaking the membrane patches. These data suggested that the absence of an unsaturation or the presence of more than one unsaturation leads to a lack of activation of TRPV1 by lipids with these structural features.

Using an overlay assay, we detected an interaction of LPA 18:1, LPA 18:2, and the fatty alcohol thiophosphate FAP-7 can also interact with TRPV1 (Fig. 1, *F* and *G*). However, this interaction does not ensure changes in the function of TRPV1, supporting the idea that lipid-protein interactions that lead to activation of the channel depend tightly on the structural features of the lipid.

We then tested another commercially available saturated lipid, CPA 16:0, and two naturally occurring unsaturated lipids, CPA 18:1 that is found in serum (31) and dioleoylglycerophosphate (DGPP) that is found in plants and yeast (32–34). When CPA 16:0 (5 μM) was applied to inside-out excised membrane patches from HEK293 cells expressing TRPV1, it did not produce TRPV1 current activation (Fig. 2, *A* and *D*). However, CPA 18:1 (5 μM) produced currents of a similar magnitude at a saturating capsaicin concentration (4 μM) (Fig. 2, *B* and *D*), and the dose-response to this lipid yielded a $K_{½}$ of 2.7 μM. However, when DGPP 18:1 with two oleyl chains was applied to these TRPV1-expressing membrane patches, no activation was observed (Fig. 2, *C* and *D*). Moreover, using an overlay assay, we also determined an interaction of the activator CPA 18:1 with TRPV1 (Fig. 2, *E* and *F*). The overlay assays also showed that DGPP 18:1 interacted with TRPV1. However, even though DGPP 18:1 bound to TRPV1, this interaction did not result in channel activation.

Thus, the data shown in Figs. 1 and 2 demonstrated that unsaturated mono-oleoylglycerophosphates were capable of activating TRPV1, whereas a dioleoylglycerophosphate was ineffective in promoting the opening of TRPV1.

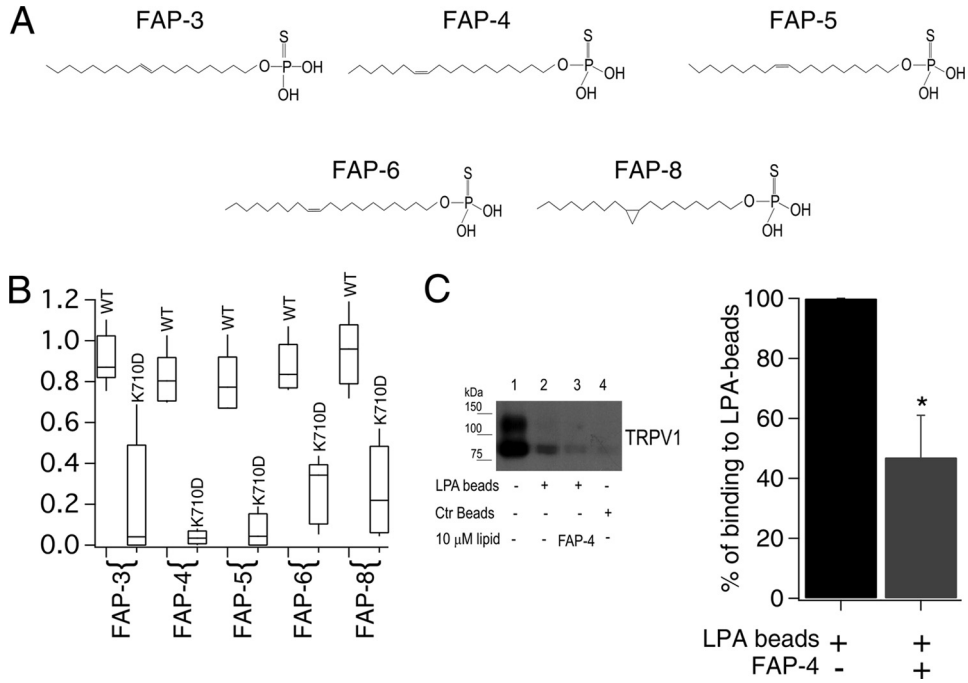

FIGURE 3. **Synthetic long-acyl chain monounsaturated lipids activate TRPV1.** *A,* monounsaturated thiophosphates FAP-3, FAP-4, FAP-5, FAP-6, and the cyclopropyl thiophosphate FAP-8. *B,* box-plot of the activation of WT TRPV1 and K710D mutant channels by the different lipids. The *horizontal line* within each box indicates the median; *boxes* show the 25th and 75th percentiles, and *whiskers* show the 5th and 95th percentiles of the data obtained at +120 mV and normalized to activation by 4 μM capsaicin ($n = 5$ and 6 for FAP-4, 6 and 5 for FAP-5, 5 and 5 for FAP-6, 16 and 15 for FAP-3, 5 and 5 for FAP-8, respectively, for WT and TRPV1-K710D). *C,* (*left panel*) pulldown assay on plasma membrane protein using LPA-coated beads from HEK293 cells transiently expressing TRPV1. *Lane 1* is protein input; *lane 2* is TRPV1 pulled down with LPA-coated beads; *lane 3* is competition with the FAP-4 lipid; and *lane 4* is pulled down protein with control beads (non-LPA-coated beads). *Bar chart* (*right panel*) for the average decrease in percentage of binding to LPA beads (obtained after analyzing the intensity of bands as the ones shown in the *left panel*) before (*black*) and after (*gray*) competition in the presence of FAP-4 is shown. Data were normalized to the intensity of the bands obtained only with LPA-coated beads. $n = 3$; *, $p < 0.02$ (Student's *t* test).

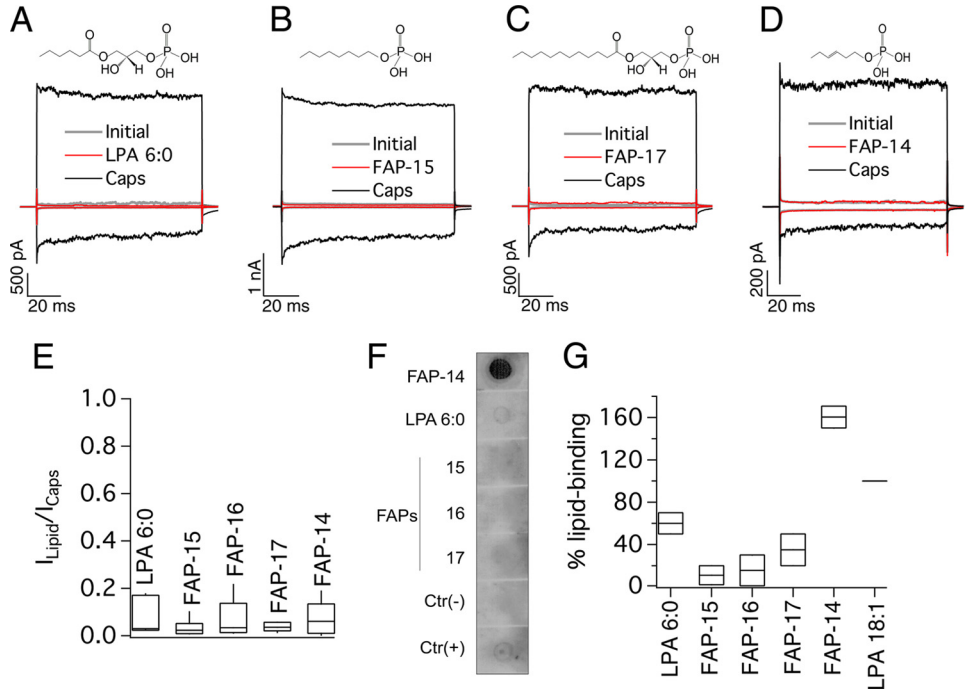

FIGURE 4. **Short-chain lipids do not activate TRPV1.** All representative traces were obtained at −120 and +120 mV. *A,* initial (in the absence of agonist, *gray*), after 5 min of 5 μM LPA 6:0 (*red*), and after 4 μM capsaicin (*Caps, black*). *B,* initial currents are in *gray*, after 5 μM FAP-15 (*red*), and after 4 μM capsaicin (*Caps, black*). *C,* initial currents are in *gray*, after 5 min of 5 μM of FAP-17 (*red*), and after 4 μM capsaicin (*Caps, black*). *D,* initial currents (*gray*) in the presence of a concentration of 5 μM monounsaturated FAP-14 for 5 min (*red*) and after 4 μM capsaicin (*Caps, black*). *E, horizontal line* within each box indicates the median; *boxes* show the 25th and 75th percentiles, and *whiskers* show the 5th and 95th percentiles of the data obtained at +120 mV and normalized to activation by 4 μM capsaicin. Data for all short-chain LPA molecules synthesized are depicted ($n = 5$ for LPA 6:0; 6 for FAP-15, FAP-16, FAP-17, and FAP-14). *F,* overlay assay for LPA 6:0 and FAP-15, -16, -17, and -14. FAP-14 clearly interacts with TRPV1, whereas fainter signals (or the lack of them) are observed for LPA 6:0 and FAP-15–17. The negative control was LPA 18:0 and the positive control was LPA 18:1. *G,* densitometry was performed for the different lipid spots and normalized with respect to the positive control (LPA 18:1). Data are shown as in *E* ($n = 2$).

Synthetic Monounsaturated Fatty Alcohol Phosphates Activate TRPV1—To evaluate the role of the glycerol backbone in TRPV1 activation, we synthesized 16 fatty alcohol phosphate and thiophosphate compounds (FAPs) (Table 1) that shared long hydrocarbon chains (18–20 carbons) with one double bond located at position 9, 10, or 11. Fig. 3 shows that FAP-3, FAP-4, FAP-5, and FAP-6 all activated TRPV1 with an efficiency similar to that of 4 μM capsaicin as measured by $I_{lipid}/I_{max\ capsaicin}$ (Fig. 3*B*). Interestingly, compound FAP-8, which presents a cyclopropyl group at position 9, also activated TRPV1 with similar efficiency as 4 μM capsaicin (Fig. 3*B*). FAP-10 with a branched hydrocarbon side chain was inactive (data not shown; see Table 1 for structure). These results point to a possible role of a region that can provide a certain degree of torsion to the molecule (*i.e.* unsaturation and a cyclopropyl group) (35) in the specificity for activation of TRPV1 by these lipids.

We had previously shown that LPA interacts with the Lys-710 residue in the C terminus of TRPV1 (9). We used the K710D mutant TRPV1 channel to determine whether these compounds interact with the same site in the C terminus as LPA 18:1 does to activate the channel. As shown in Fig. 3*B*, all of the compounds tested showed a clear decrease in the activation of the mutant TRPV1 channel as compared with the WT TRPV1 channel.

Moreover, as demonstrated previously (9), we found that the TRPV1 channel interacts with LPA-coated beads in pulldown assays (Fig. 3*C*, *lane 2*). In addition, when TRPV1 was preincubated with one of the fatty alcohol phosphates described above, FAP-4, the amount of channel pulled down by the LPA-coated beads was greatly diminished (Fig. 3*C*, *lane 3*), also indicating that lipid FAP-4 competes for the same site that LPA 18:1 binds to in the proximal C terminus of TRPV1.

Lipid Analogs with Dodecanoyl or Shorter Hydrocarbon Chains Fail to Activate TRPV1—We have previously shown that LPA binds to the proximal region of the C terminus of TRPV1 through a mechanism that partly involves electrostatic interactions, presumably with the charged phosphate group of LPA and the charged Lys-710 residue of TRPV1. Under this scenario, the hydrophobic acyl chain of LPA would be inserted in the membrane or buried in the membrane-protein interface with its polar headgroup facing the cytoplasmic side interacting with Lys-710. Hence, we hypothesized that changes in the length of the acyl chain of LPA may curtail the effect of this lipid on TRPV1 activity.

To test the latter possibility, we purchased a short-chain LPA and synthesized short-chain FAPs that ranged from aliphatic chain lengths of 6–12 carbons. In this case, neither LPA 6:0, FAP-15, FAP-16, nor FAP-17 (see Table 1 and Fig. 4) produced activation of TRPV1 currents (Fig. 4, *A–D, red traces,* and *E*) as compared with activation by capsaicin. Moreover, we tested whether these lipids could bind to TRPV1, and the representative biochemical assay shown in Fig. 4, *F* and *G,* is indicative of either a weak or a complete lack of interaction of these short-chain lipids with the channel. However, the aforementioned lipids are not only molecules with short chains but these chains are also saturated, a trait that was also distinctive from those lipids that activate TRPV1 as shown in Fig. 1.

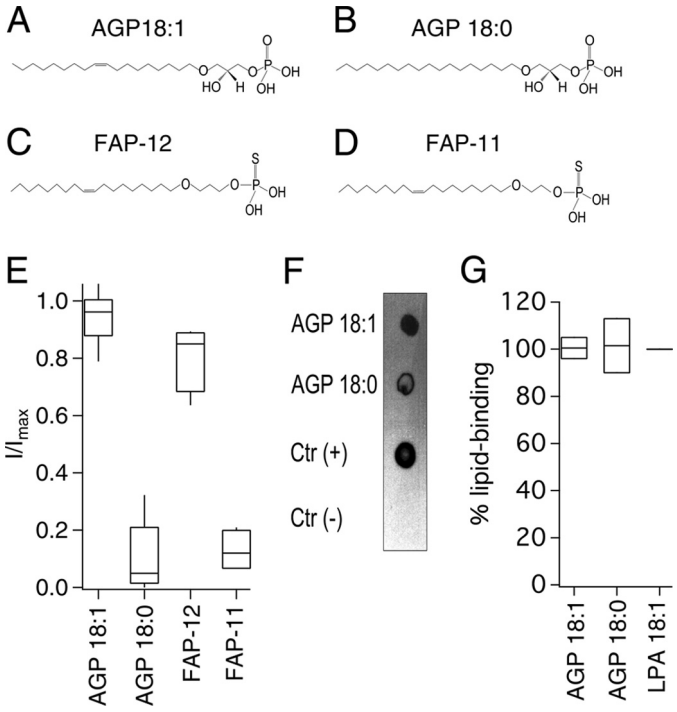

FIGURE 5. **Specificity of activation of TRPV1 by alkyl lipids.** *A–D,* chemical structures of AGP18:1 (*A*) and AGP18:0 (*B*) of FAP-12 (*C*) and FAP-11 (*D*). *E, horizontal line* within each box indicates the median; *boxes* show the 25th and 75th percentiles, and *whiskers* show the 5th and 95th percentiles of the data percentiles of the data obtained at +120 mV and normalized to activation by 4 μM capsaicin (n = 6 for AGP 18:1; 5 for AGP 18:0; and 4 for FAP-12 and FAP-11). *F,* overlay assay shows that AGP 18:1 and AGP 18:0 bind to TRPV1. LPA 18:1 was the positive control indicated as *Ctr* (+) and DMEM with 1% fatty acid-free BSA was used as a negative control indicated as *Ctr* (−). *G,* densitometry was performed for the different lipid spots and normalized with respect to the positive control (LPA 18:1). Data are shown as in *E* (n = 2).

Because double bonds provide a considerable degree of torsion and motion to the fatty acid chains (35), which may be important for proper physical interaction with a site in the ion channel, we synthesized the Δ4-monounsaturated hexyl chain FAP-14 and tested whether it could activate TRPV1 by applying this lipid to the intracellular face of the channel. The results in Fig. 4, *D* (*red trace*) and *E,* show that FAP-14 failed to induce TRPV1-mediated currents, as the currents in the presence of this lipid were indistinguishable from those obtained initially in the absence of chemical ligands. Moreover, we performed overlay assays to determine whether there was an interaction of FAP-14 with TRPV1 and found that in fact it did bind to the channel (Fig. 4, *F* and *G*). Thus, these data indicated that the presence of an unsaturation at position Δ4 in a short-chain lipid did not render it functionally relevant as an agonist of TRPV1, although it could interact with the protein.

Other Structural Requirements for the Activation of TRPV1 by Long-chain Lipids—To this point, using lipids similar to LPA, we have shown that a long chain and the presence of one unsaturation or a torsion-providing cyclopropyl group are necessary for the activation of TRPV1. We now sought to determine whether lipids with an ether link instead of an ester link between the hydrocarbon chain and the glycerol backbone could also promote TRPV1 activation. For this purpose, we also used two commercially available alkyl lipids (AGP 18:1 and AGP 18:0), and we synthesized another two similar ether-

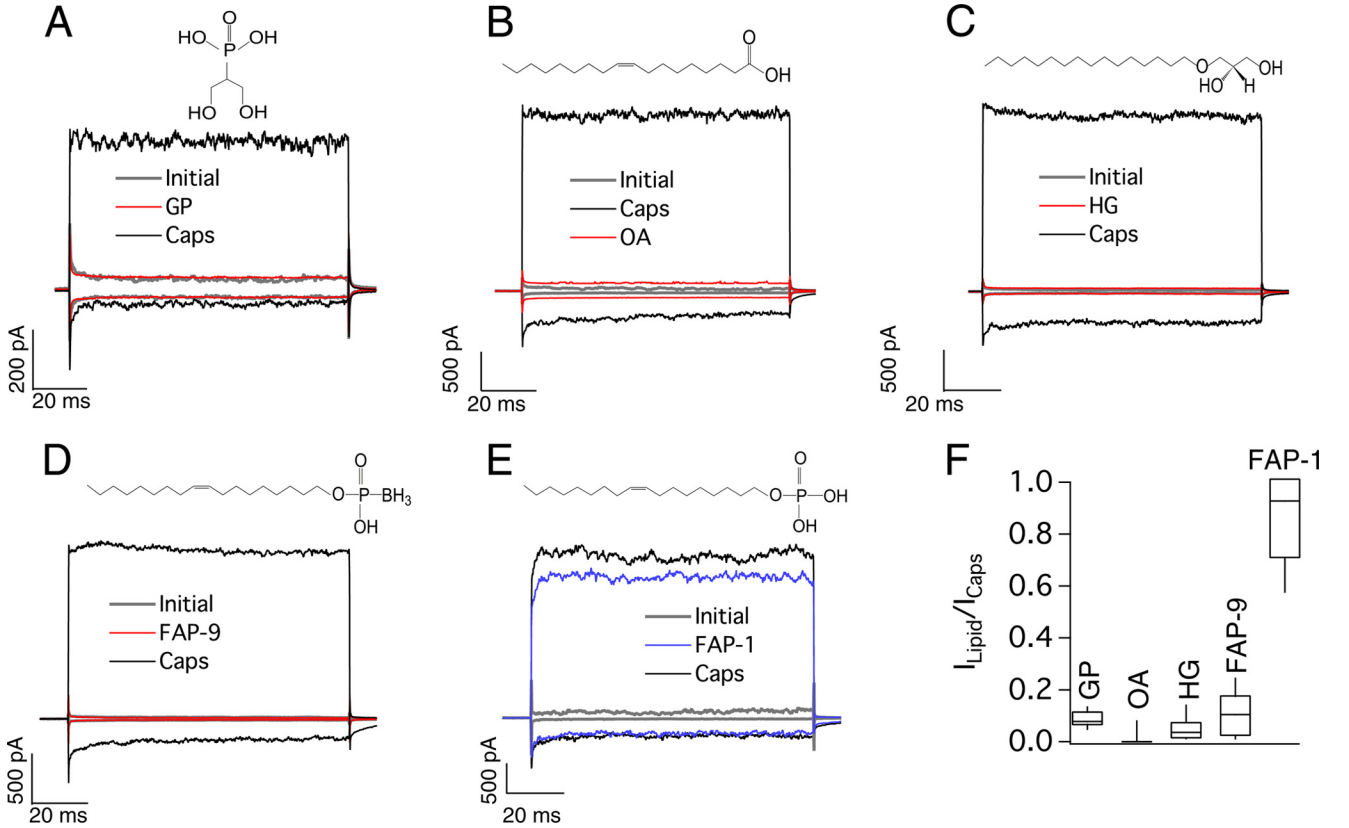

FIGURE 6. **Compounds that do not activate TRPV1.** *A,* representative traces obtained at −120 and +120 mV initially (leak, *gray*), after 5 min of 5 μM glycerol phosphate (*GP*; *red*), and after 4 μM capsaicin (*Caps, black*). *B,* traces obtained as in *A* initially (*gray*), after 4 μM capsaicin (*black*) and after wash and 5 μM oleic acid (*OA*; *red*), and *C, traces* as in *A* and *B*. Initial currents are in *gray,* after 5 min of 5 μM of 1-C16 ether MG 1-*O*-hexadecyl-*sn*-glycerol (*HG*, *red*), and after 4 μM capsaicin (*black*). *D,* traces as in *A–C*. Initial currents are in *gray*, after 5 μM of FAP-9 in *red,* and after 4 μM capsaicin (*black*). *E,* traces as in *A–C*. Initial currents are in *gray*, after 5 μM of FAP-1 in *blue,* and after 4 μM capsaicin (*black*). *F, horizontal line* within each box indicates the median; *boxes* show the 25th and 75th percentiles, and *whiskers* show the 5th and 95th percentiles of the data obtained at +120 mV and normalized to activation by 4 μM capsaicin. None of these compounds, except FAP-1, activated TRPV1 ($n = 6$ for glycerol phosphate, 11 for oleic acid, 6 for glycerol phosphate, 5 for FAP-9, and 6 for FAP-1).

linked compounds, FAP-11 and FAP-12, that differed from each other in the position of the ether with respect to the thiophosphate headgroup. When TRPV1-expressing membrane patches from HEK293 cells were exposed to AGP 18:1 (Fig. 5, *A* and *E*), we found that the channel activated similarly to what we observed with LPA 18:1 (Fig. 1*A*). In contrast, TRPV1 currents could not be activated by the application of AGP 18:0 (Fig. 5, *B* and *E*), reinforcing the hypothesis that the presence of an unsaturation is required for activation of the channel. Moreover, we once again found that a lipid such as AGP 18:0 that does not activate the channel can bind to TRPV1 (Fig. 5*F*).

Interestingly, although the FAP-12 compound clearly activated TRPV1 (Fig. 5, *C* and *E*), the FAP-11 compound, at a concentration of 5 μM, failed to induce TRPV1-mediated currents (Fig. 5, *D* and *E*), indicating that the position of the ether bond with respect to the negatively charged headgroup is also important. However, when we tested FAP-11 at a concentration of 25 μM, we were able to observe nearly 80% of activation of the TRPV1 channel as compared with a saturating concentration of capsaicin (Table 1), indicating that although less effective than FAP-12, FAP-11 can induce channel activation at high concentrations.

Then we decided to test whether the glycerol phosphate (which contains the charged headgroup; Fig. 6*A*) oleic acid (an unsaturated 18-carbon acyl chain without a charged headgroup; Fig. 6*B*) or whether 1-*O*-hexadecyl glycerol (a saturated 16-carbon alkyl chain ether without a charged headgroup; Fig. 6*C, HG*) could influence TRPV1 activity on their own. In summary, we found that none of these compounds could promote TRPV1 function (Fig. 6, *A–C, red traces,* and *F*), demonstrating that these different component parts of lipids alone are not structurally sufficient for activation of TRPV1.

To further probe the role of the negatively charged headgroup, we synthesized the fatty alcohol analog FAP-9 with a boron phosphate and a hydrocarbon chain of 18 carbons with monounsaturation at the Δ9 position. This compound was ineffective in activating the channel (Fig. 6, *D, red trace*, and *F*), suggesting that a variation in the electronegativity of the charged headgroup is responsible for this observation. Moreover, a compound similar to FAP-9 but without the boron phosphate group, FAP-1, was able to activate TRPV1 (Fig. 6, *E* and *F*).

Finally, we had previously shown that the LPA G-protein-coupled receptor (GPCR) pan-antagonist BrP-LPA (9, 36) is an activator of TRPV1, despite the fact that it has a saturated acyl chain. This observation is contrary to the findings we presented above for a host of compounds demonstrating a strict requirement for a single double bond in the hydrocarbon chain of active ligands.

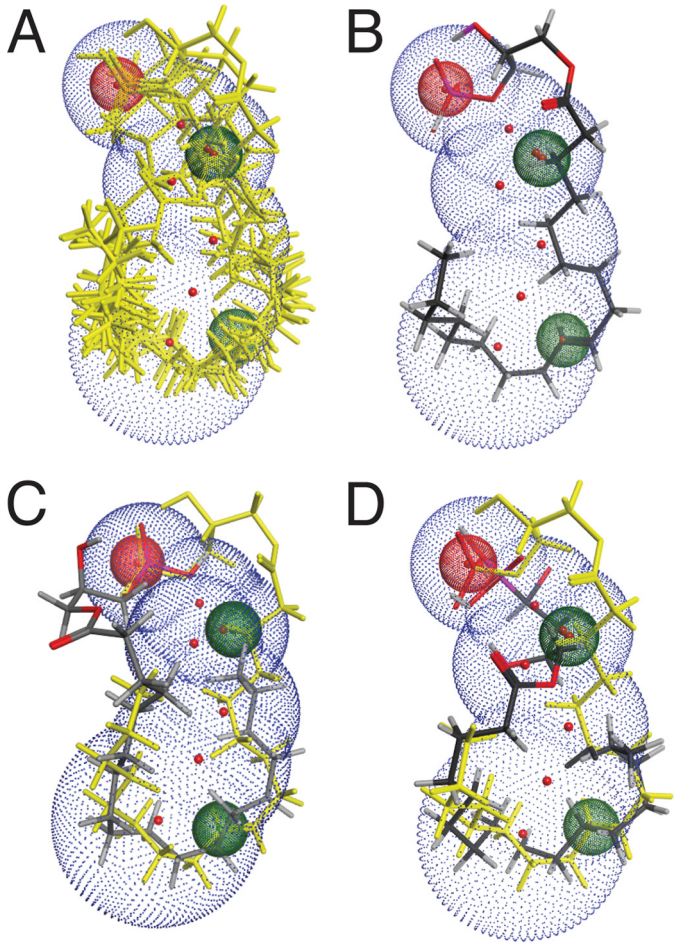

FIGURE 7. **Ligand-based pharmacophore of TRPV1 activation reveals three key features.** *A,* three-dimensional alignment of the active compounds (*yellow*). Three-point pharmacophore query modeled on the bioactive conformation of active compounds: the anionic group with two hydrophobic features. *B,* LPA 18:1 shown as representative of the ability of unsaturated compounds to adopt an active conformation. *C,* superimposition of LPA 18:1 (*yellow*) and LPA 18:0 (*stick*) reveals that LPA 18:1 occupies the three pharmacophore features, whereas LPA 18:0 is unable to extend to the critical hydrophobic intersection. *D,* flexible alignment of LPA 18:1 (*yellow*) and BrP-LPA (*stick*) indicates that a similar low energy conformation can be adopted, although the two compounds curl in opposite ways.

To resolve this apparent contradiction between our present results showing that ligands only with a single double bond are effective activators of TRPV1, all active compounds were superimposed using the "flexible alignment" procedure implemented in MOE (MOE 2011.08 version, Chemical Computing Group Inc., Montreal, Quebec, Canada). A ligand-based pharmacophore consisting of an anionic headgroup and two hydrophobic groups (Fig. 7, *red* and *green dots*) highlights key features shared by all of the active compounds. All active compounds were able to adopt a conformation that the inactive compounds do not. In addition to the negatively charged headgroup, the two hydrophobic points where the active compounds intersect appear to be critical for activity. In Fig. 7*A*, an overlay of all active compounds is shown. As an example, LPA 18:1 (Fig. 7*B*) shares all three features defined by the overlay of all active ligands in Fig. 7*A*. In contrast, in the case of the inactive LPA 18:0, whose superimposition with LPA 18:1 is shown in Fig. 7*C*, the hydrocarbon chain bends away from the middle point of the pharmacophore. Surprisingly, BrP-LPA (Fig. 7*D*), although saturated, is predicted to cross the middle hydrophobic feature similarly to the unsaturated active compounds. The bromophosphonate headgroup appears to push its hydrophobic feature in the middle closer to the end of the hydrocarbon tail. However, BrP-LPA curls from left to right instead of the predicted right to left curl in LPA 18:1 (Fig. 7, *B* and *D*). All of the above support the hypothesis that the hydrophobic feature in the middle of the pharmacophore and the nature of the negatively charged headgroup together play an important role in defining activity.

DISCUSSION

We have shown previously that the TRPV1 channel is activated by LPA 18:1. This was the first description of a direct interaction of LPA, a molecule implicated in neuropathic pain, with a TRP channel that importantly mediates noxious signals (9).

In light of these previous findings and other recent studies showing that negatively charged lipids can positively regulate the activity of TRPV1 channels (16–18, 20), we sought to determine the structural requirements that lipids and compounds similar to LPA have to meet to elicit TRPV1 activation. For this purpose, we used a variety of naturally occurring and synthetic analogs to discern their requirements for TRPV1 activation.

By varying the chain lengths, unsaturations, their positions, and their headgroups, we were able to identify several lipids that activate TRPV1 (AGP 18:1, CPA 18:1, and FAP-1–9) in a similar fashion to LPA 18:1 (see Table 1). Moreover, we tested (37, 38) whether the endogenously produced lipid CPA 18:1 could bind to the protein in biochemical assays, and we found that it does bind to the TRPV1 channel. The effects of long acyl chain lipids on ion channel regulation is not unique for the TRPV1 channels (16), but it has also been described for K_{ATP} ion channels (39), large conductance Ca^{2+} potassium (BK) channels (40), and inwardly rectifying potassium (Kir) channels (41). However, short-chain LPAs, saturated or monounsaturated, did not activate TRPV1. Based on these observations, we hypothesized that the chain length might be important because the acyl chain could interact directly with the core of the protein, whereas the phosphate group interacts with charged residues in the association domain, including Lys-710, a residue previously shown to form part of a binding site for LPA (9).

Our results using AGP and the FAP series indicate that the chemical bond linking the headgroup to the hydrocarbon chain can be either an ester or an ether bond, and TRPV1 activation is still achieved. We also determined that the glycerol backbone is not essential for TRPV1 activity. The negatively charged headgroup can be a phosphate, thiophosphate, or cyclic phosphate (Table 1). However, the boron phosphate does not elicit TRPV1 activation. Single double bonds in positions Δ9, 10 or 11 of the hydrocarbon chain, in either *cis* or *trans* configuration or a cyclopropyl group in the Δ9 position, were all tolerated and active. The ligand-based pharmacophore identified three features shared by all active compounds. Our data support the ionic interaction between the negatively charged headgroup with Lys-710 in the proximal C terminus, as shown by the decreased effect of the FAP compounds with the K710D TRPV1

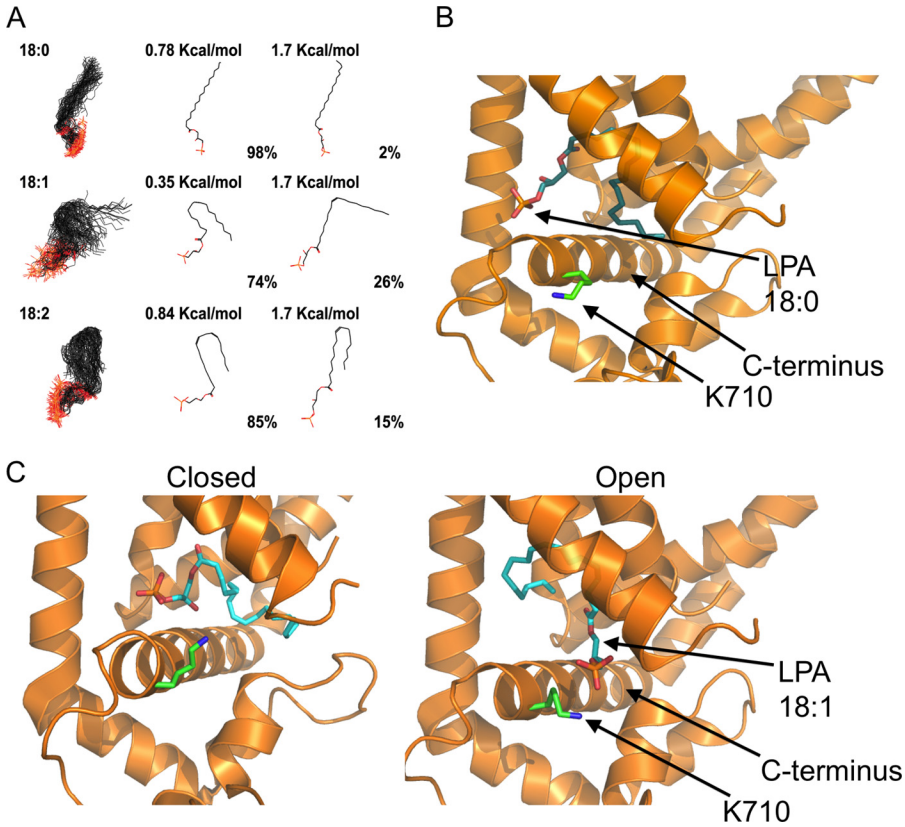

FIGURE 8. **Proposed mechanism for activation of TRPV1 by long-chain lipids.** *A,* LPA 18:0, 18:1, and 18:2 were modeled to simulate an aqueous environment using a Monte Carlo conformational analysis. *1st panel* shows all the conformations that may be adopted by the different lipids; *2nd panel* shows the conformation adopted under minimal energy requirements; and *3rd panel* shows the conformation adopted under a chosen high energy condition. The percentage of molecules found in a given conformation under a certain energetic condition are indicated below the molecules in the *2nd* and *3rd panels*. *B,* docking of LPA 18:0 in the minimal energy conformation shown in *2nd panel* (0.78 kcal/mol) to the published cryo-EM structure of TRPV1. In this proposed model, there is a lack of interaction of the negatively charged phosphate group of LPA 18:0 with the Lys-710 residue (*green*) in the proximal C terminus of TRPV1. The structure of LPA 18:0 (*cyan*) is shown docked to the open state of the channel. *C,* docking of LPA 18:1 in the minimal energy conformation shown in *2nd panel* (0.35 kcal/mol) to the published cryo-EM structure of TRPV1. During opening of the channel, the proximal C terminus helix of TRPV1 could move parallel to the plasma membrane (compare panels on the *left* for closed state (PDB code 3J5P-B) and on the *right* for open state (PDB code 3J5Q-D). In this proposed model, interaction of the negatively charged phosphate group with the Lys-710 residue (*green*) in the proximal C terminus of TRPV1 would lead to the open conformational change by promoting movement of the C-helix. The docked structure of LPA 18:1 (*cyan*) is shown in both the closed and open states.

mutant channel. Nonetheless, it is possible that they have a complex binding site, and they also interact with other residues in the ion channel because some of these compounds displayed more current activation of the TRPV1-K710D mutant than what we had previously reported for LPA 18:1 (9). Moreover, we do not know which part of the channel protein interacts with the hydrocarbon chain. Identification of this interaction site awaits further investigation. We also find that the structural determinants for activation of the TRPV1 channel by the lipids studied here are far more restricted for LPA species than that of the LPA GPCRs. LPA GPCRs are activated by several analogs that were ineffective at activating TRPV1, including short-chain LPAs with C10–12 carbons and saturated or polyunsaturated LPA species with chain lengths ≥18.

In the acetylcholine receptor, it has been shown that the position of the double bond in monounsaturated free fatty acids is pivotal for the inhibitory effects of these lipids on the receptor channel (42). By studying the effects of having a double bond at different positions, Perillo *et al.* (42) determined that only those in positions ω6 and ω9 could exert changes in the open probability of the receptor channel. From these results, it was concluded that the position and isomerism of the torsion angle of unsaturated free fatty acids are important for their role as inhibitors of the acetylcholine receptor.

Here, we have tested long-chain molecules with none, one, or two double bonds on the activation of TRPV1. We find that neither LPA 18:0 nor LPA 18:2 (not even at concentrations as high as 25 μM) could activate the channel. Previous studies have shown that, for the case of C18 *N*-acylethanolamines, the presence of two unsaturations renders these molecules more effective as agonists of TRPV1 (27). The unsaturation of LPA 18:1 provides an increase in the rate of motion and a decrease in the order of the acyl chain (35), probably allowing it to gain a conformation suitable for interaction with amino acids in a hydrophobic pocket in the transmembrane region of the channel. However, because DGPP 18:1 could not activate TRPV1, it is possible that the hydrophobic pocket with which LPA 18:1 interacts is unable to accommodate two fatty acid chains.

Lipids that possess different degrees of unsaturation acquire different structures. As can be seen from the modeling of the lipids in Fig. 8*A*, the LPA 18:0 structure is linear, whereas the LPA 18:1 and LPA 18:2 molecules acquire different degrees of torsion. It is also possible that the presence of an unsaturation

in the aliphatic chain of a lipid not only provides the right degree of torsion but also provides the ability to establish a π-electron bond with an aromatic residue (43) located in the transmembrane region of the channel, stabilizing the lipid-protein interaction.

It has been suggested that the polyunsaturated LPA species 18:2 and 20:4 and the monounsaturated 18:1 constitute the majority of the LPA in serum with 38, 39, and 9%, respectively (44). Using an animal model where nerve injury was experimentally induced, it was previously determined that the levels of 18:1, 16:0, and 18:0 LPA in the spinal dorsal horn are increased (45). In this model, it was shown that LPA 18:1 is the major species of LPA in quantity and the most relevant species in pain generation (45).

For other channels, lipid-protein interactions have been proposed. For example, for the Kir 2.2 channel there is an x-ray crystal structure of the protein in the presence of PIP_2. Hansen *et al*. (46) found that PIP_2 binds at an interface between the transmembrane domain and a nonspecific phospholipid-binding region in the cytoplasmic domain. When PIP_2 binds, there is contraction of a flexible expansion linker that changes this region into a compact helical structure (46). This could be a similar scenario to what happens with LPA and TRPV1.

Fig. 8*B* shows an example of a lipid-protein interaction between LPA 18:0 (that does not activate the channel) and TRPV1. In this case, the hypothesis is that the charged phosphate headgroup of LPA 18:0 is not correctly oriented and thus is incapable of interacting with Lys-710.

In a recently obtained cryostructure of the TRPV1 channel, the Lys-710 residue in the proximal C terminus of the channel (located near the TRP box) moves parallel to the axis of the membrane when the channel is in an activated state (Fig. 8*C*) with either capsaicin or resiniferatoxin and double-knot toxin as compared with the apo-state (47). Here, we propose that long-chain LPA-like molecules of 18 carbons with one double bond at the pharmacophore feature (Fig. 7), which provides a "kink" to the lipids, adopt a conformation that promotes that the positively charged Lys-710 residue moves parallel to the membrane to be able to interact with the charged headgroup, causing a conformational change that can render TRPV1 active (Fig. 8*C*, *right*).

In our biochemical assays, we found that lipids that did not activate TRPV1 could still bind to the channel (*e.g.* FAP-14 and DGPP 18:1), probably through their interaction with other charged residues in the protein. However, the fact that these lipids could not affect TRPV1 function shows that not all interactions of lipids with the channel lead to a change in its function, similar to what happens with the Kir2.2 channel (48). We interpret these findings as indicating that binding to and activation of the channel represent two distinct events in the lipid-protein interaction of TRPV1.

We propose that the binding of the 18:1 fatty acid of LPA in a hydrophobic pocket of the channel and the electrostatic attraction of Lys-710 produce a distortion/conformational change in the association domain that is transduced to the pore segments and the gating machinery, triggering the channel to open. Our data are in accordance with previous findings that, in excised membrane patches, lipids positively regulate the activity of TRPV1.

Acknowledgments—We especially thank Felix Sierra for expert assistance with some patch clamp experiments. We thank Lorenzo Sánchez Vásquez for some initial experiments. We also thank Laura Ongay, Ana Escalante, Francisco Pérez, and Valeria Martínez at Instituto de Fisiología Celular, Universidad Nacional Autónoma de México, for technical support. We thank Dr. Abby Parrill for the access to MOE by the Chemical Computing Group supplied to the University of Memphis, Department of Chemistry, and Jin Emerson-Cobb for editing the manuscript.

REFERENCES

1. Vay, L., Gu, C., and McNaughton, P. A. (2012) The thermo-TRP ion channel family: properties and therapeutic implications. *Br. J. Pharmacol.* **165,** 787–801
2. Moran, M. M., McAlexander, M. A., Bíró, T., and Szallasi, A. (2011) Transient receptor potential channels as therapeutic targets. *Nat. Rev. Drug Discov.* **10,** 601–620
3. Engler, A., Aeschlimann, A., Simmen, B. R., Michel, B. A., Gay, R. E., Gay, S., and Sprott, H. (2007) Expression of transient receptor potential vanilloid 1 (TRPV1) in synovial fibroblasts from patients with osteoarthritis and rheumatoid arthritis. *Biochem. Biophys. Res. Commun.* **359,** 884–888
4. Pan, H. L., Zhang, Y. Q., and Zhao, Z. Q. (2010) Involvement of lysophosphatidic acid in bone cancer pain by potentiation of TRPV1 via PKCϵ pathway in dorsal root ganglion neurons. *Mol. Pain* **6,** 85
5. Sadofsky, L. R., Ramachandran, R., Crow, C., Cowen, M., Compton, S. J., and Morice, A. H. (2012) Inflammatory stimuli up-regulate transient receptor potential vanilloid-1 expression in human bronchial fibroblasts. *Exp. Lung Res.* **38,** 75–81
6. Caterina, M. J., Schumacher, M. A., Tominaga, M., Rosen, T. A., Levine, J. D., and Julius, D. (1997) The capsaicin receptor: a heat-activated ion channel in the pain pathway. *Nature* **389,** 816–824
7. Hwang, S. W., Cho, H., Kwak, J., Lee, S. Y., Kang, C. J., Jung, J., Cho, S., Min, K. H., Suh, Y. G., Kim, D., and Oh, U. (2000) Direct activation of capsaicin receptors by products of lipoxygenases: endogenous capsaicin-like substances. *Proc. Natl. Acad. Sci. U.S.A.* **97,** 6155–6160
8. Morales-Lázaro, S. L., Simon, S. A., and Rosenbaum, T. (2013) The role of endogenous molecules in modulating pain through transient receptor potential vanilloid 1 (TRPV1). *J. Physiol.* **591,** 3109–3121
9. Nieto-Posadas, A., Picazo-Juárez, G., Llorente, I., Jara-Oseguera, A., Morales-Lázaro, S., Escalante-Alcalde, D., Islas, L. D., and Rosenbaum, T. (2012) Lysophosphatidic acid directly activates TRPV1 through a C-terminal binding site. *Nat. Chem. Biol.* **8,** 78–85
10. Lin, M. E., Herr, D. R., and Chun, J. (2010) Lysophosphatidic acid (LPA) receptors: signaling properties and disease relevance. *Prostaglandins Other Lipid Mediat.* **91,** 130–138
11. Baker, D. L., Desiderio, D. M., Miller, D. D., Tolley, B., and Tigyi, G. J. (2001) Direct quantitative analysis of lysophosphatidic acid molecular species by stable isotope dilution electrospray ionization liquid chromatography-mass spectrometry. *Anal. Biochem.* **292,** 287–295
12. Choi, J. W., Herr, D. R., Noguchi, K., Yung, Y. C., Lee, C. W., Mutoh, T., Lin, M. E., Teo, S. T., Park, K. E., Mosley, A. N., and Chun, J. (2010) LPA receptors: subtypes and biological actions. *Annu. Rev. Pharmacol. Toxicol.* **50,** 157–186
13. Ueda, H., Matsunaga, H., Olaposi, O. I., and Nagai, J. (2013) Lysophosphatidic acid: chemical signature of neuropathic pain. *Biochim. Biophys. Acta* **1831,** 61–73
14. Inoue, M., Rashid, M. H., Fujita, R., Contos, J. J., Chun, J., and Ueda, H. (2004) Initiation of neuropathic pain requires lysophosphatidic acid receptor signaling. *Nat. Med.* **10,** 712–718
15. Lukacs, V., Thyagarajan, B., Varnai, P., Balla, A., Balla, T., and Rohacs, T. (2007) Dual regulation of TRPV1 by phosphoinositides. *J. Neurosci.* **27,** 7070–7080

16. Lukacs, V., Rives, J. M., Sun, X., Zakharian, E., and Rohacs, T. (2013) Promiscuous activation of transient receptor potential vanilloid 1 (TRPV1) channels by negatively charged intracellular lipids: the key role of endogenous phosphoinositides in maintaining channel activity. *J. Biol. Chem.* **288,** 35003–35013
17. Ufret-Vincenty, C. A., Klein, R. M., Hua, L., Angueyra, J., and Gordon, S. E. (2011) Localization of the PIP2 sensor of TRPV1 ion channels. *J. Biol. Chem.* **286,** 9688–9698
18. Senning, E. N., Collins, M. D., Stratiievska, A., Ufret-Vincenty, C. A., and Gordon, S. E. (2014) Regulation of TRPV1 by phosphoinositide (4,5)-bisphosphate: role of membrane asymmetry. *J. Biol. Chem.* **289,** 10999–11006
19. Cao, E., Cordero-Morales, J. F., Liu, B., Qin, F., and Julius, D. (2013) TRPV1 channels are intrinsically heat sensitive and negatively regulated by phosphoinositide lipids. *Neuron* **77,** 667–679
20. Stein, A. T., Ufret-Vincenty, C. A., Hua, L., Santana, L. F., and Gordon, S. E. (2006) Phosphoinositide 3-kinase binds to TRPV1 and mediates NGF-stimulated TRPV1 trafficking to the plasma membrane. *J. Gen. Physiol.* **128,** 509–522
21. Klein, R. M., Ufret-Vincenty, C. A., Hua, L., and Gordon, S. E. (2008) Determinants of molecular specificity in phosphoinositide regulation. Phosphatidylinositol (4,5)-bisphosphate ($PI(4,5)P_2$) is the endogenous lipid regulating TRPV1. *J. Biol. Chem.* **283,** 26208–26216
22. Telezhkin, V., Reilly, J. M., Thomas, A. M., Tinker, A., and Brown, D. A. (2012) Structural requirements of membrane phospholipids for M-type potassium channel activation and binding. *J. Biol. Chem.* **287,** 10001–10012
23. Telezhkin, V., Brown, D. A., and Gibb, A. J. (2012) Distinct subunit contributions to the activation of M-type potassium channels by $PI(4,5)P_2$. *J. Gen. Physiol.* **140,** 41–53
24. Gududuru, V. (April 1, 2014) U. S. Patent 8, 686,177 B2
25. Durgam, G. G., Virag, T., Walker, M. D., Tsukahara, R., Yasuda, S., Liliom, K., van Meeteren, L. A., Moolenaar, W. H., Wilke, N., Siess, W., Tigyi, G., and Miller, D. D. (2005) Synthesis, structure-activity relationships, and biological evaluation of fatty alcohol phosphates as lysophosphatidic acid receptor ligands, activators of PPARγ, and inhibitors of autotaxin. *J. Med. Chem.* **48,** 4919–4930
26. Rosenbaum, T., and Gordon, S. E. (2002) Dissecting intersubunit contacts in cyclic nucleotide-gated ion channels. *Neuron* **33,** 703–713
27. Movahed, P., Jönsson, B. A., Birnir, B., Wingstrand, J. A., Jørgensen, T. D., Ermund, A., Sterner, O., Zygmunt, P. M., and Högestätt, E. D. (2005) Endogenous unsaturated C18 *N*-acylethanolamines are vanilloid receptor (TRPV1) agonists. *J. Biol. Chem.* **280,** 38496–38504
28. Brauchi, S., Orta, G., Mascayano, C., Salazar, M., Raddatz, N., Urbina, H., Rosenmann, E., Gonzalez-Nilo, F., and Latorre, R. (2007) Dissection of the components for PIP2 activation and thermosensation in TRP channels. *Proc. Natl. Acad. Sci. U.S.A.* **104,** 10246–10251
29. Huey, R., Morris, G. M., Olson, A. J., and Goodsell, D. S. (2007) A semiempirical free energy force field with charge-based desolvation. *J. Comput. Chem.* **28,** 1145–1152
30. Seeliger, D., and de Groot, B. L. (2010) Ligand docking and binding site analysis with PyMOL and Autodock/Vina. *J. Comput. Aided Mol. Des.* **24,** 417–422
31. Kobayashi, T., Tanaka-Ishii, R., Taguchi, R., Ikezawa, H., and Murakami-Murofushi, K. (1999) Existence of a bioactive lipid, cyclic phosphatidic acid, bound to human serum albumin. *Life Sci.* **65,** 2185–2191
32. van Schooten, B., Testerink, C., and Munnik, T. (2006) Signalling diacylglycerol pyrophosphate, a new phosphatidic acid metabolite. *Biochim. Biophys. Acta* **1761,** 151–159
33. Wissing, J. B., and Behrbohm, H. (1993) Diacylglycerol pyrophosphate, a novel phospholipid compound. *FEBS Lett.* **315,** 95–99
34. Oshiro, J., Han, G. S., and Carman, G. M. (2003) Diacylglycerol pyrophosphate phosphatase in *Saccharomyces cerevisiae*. *Biochim. Biophys. Acta* **1635,** 1–9
35. Martinez-Seara, H., Róg, T., Pasenkiewicz-Gierula, M., Vattulainen, I., Karttunen, M., and Reigada, R. (2007) Effect of double bond position on lipid bilayer properties: insight through atomistic simulations. *J. Phys. Chem. B* **111,** 11162–11168
36. Xu, X., Yang, G., Zhang, H., and Prestwich, G. D. (2009) Evaluating dual activity LPA receptor pan-antagonist/autotaxin inhibitors as anti-cancer agents *in vivo* using engineered human tumors. *Prostaglandins Other Lipid Mediat.* **89,** 140–146
37. Tsukahara, T., Tsukahara, R., Fujiwara, Y., Yue, J., Cheng, Y., Guo, H., Bolen, A., Zhang, C., Balazs, L., Re, F., Du, G., Frohman, M. A., Baker, D. L., Parrill, A. L., Uchiyama, A., Kobayashi, T., Murakami-Murofushi, K., and Tigyi, G. (2010) Phospholipase D2-dependent inhibition of the nuclear hormone receptor PPARγ by cyclic phosphatidic acid. *Mol. Cell* **39,** 421–432
38. Kakiuchi, Y., Nagai, J., Gotoh, M., Hotta, H., Murofushi, H., Ogawa, T., Ueda, H., and Murakami-Murofushi, K. (2011) Antinociceptive effect of cyclic phosphatidic acid and its derivative on animal models of acute and chronic pain. *Mol. Pain* **7,** 33
39. Liu, G. X., Hanley, P. J., Ray, J., and Daut, J. (2001) Long-chain acyl-coenzyme A esters and fatty acids directly link metabolism to K(ATP) channels in the heart. *Circ. Res.* **88,** 918–924
40. Hoshi, T., Wissuwa, B., Tian, Y., Tajima, N., Xu, R., Bauer, M., Heinemann, S. H., and Hou, S. (2013) Omega-3 fatty acids lower blood pressure by directly activating large-conductance Ca^{2+}-dependent K^+ channels. *Proc. Natl. Acad. Sci. U.S.A.* **110,** 4816–4821
41. Rohács, T., Lopes, C. M., Jin, T., Ramdya, P. P., Molnár, Z., and Logothetis, D. E. (2003) Specificity of activation by phosphoinositides determines lipid regulation of Kir channels. *Proc. Natl. Acad. Sci. U.S.A.* **100,** 745–750
42. Perillo, V. L., Fernández-Nievas, G. A., Vallés, A. S., Barrantes, F. J., and Antollini, S. S. (2012) The position of the double bond in monounsaturated free fatty acids is essential for the inhibition of the nicotinic acetylcholine receptor. *Biochim. Biophys. Acta* **1818,** 2511–2520
43. Bartlett, G. J., Choudhary, A., Raines, R. T., and Woolfson, D. N. (2010) $n \rightarrow \pi^*$ interactions in proteins. *Nat. Chem. Biol.* **6,** 615–620
44. Rosenbaum, T., and Simon, S. A. (2007) in *TRP Ion Channel Function in Sensory Transduction and Cellular Signaling Cascades* (Liedtke, W. B., and Heller, S., eds) pp. 69–84, CRC Press, Inc., Boca Raton, FL
45. Ma, L., Nagai, J., Chun, J., and Ueda, H. (2013) An LPA species (18:1 LPA) plays key roles in the self-amplification of spinal LPA production in the peripheral neuropathic pain model. *Mol. Pain* **9,** 29
46. Hansen, S. B., Tao, X., and MacKinnon, R. (2011) Structural basis of PIP_2 activation of the classical inward rectifier K^+ channel Kir2.2. *Nature* **477,** 495–498
47. Cao, E., Liao, M., Cheng, Y., and Julius, D. (2013) TRPV1 structures in distinct conformations reveal activation mechanisms. *Nature* **504,** 113–118
48. Cheng, W. W., D'Avanzo, N., Doyle, D. A., and Nichols, C. G. (2011) Dual-mode phospholipid regulation of human inward rectifying potassium channels. *Biophys. J.* **100,** 620–628